



HAL
open science

Fuzzy Fault-Tolerant Predefined-Time Control for Switched Systems: A Singularity-Free Method

Di Cui, Mohammed Chadli, Zhengrong Xiang

► **To cite this version:**

Di Cui, Mohammed Chadli, Zhengrong Xiang. Fuzzy Fault-Tolerant Predefined-Time Control for Switched Systems: A Singularity-Free Method. *IEEE Transactions on Fuzzy Systems*, 2024, 32 (3), pp.1223–1232. 10.1109/TFUZZ.2023.3321688 . hal-04243143

HAL Id: hal-04243143




<https://hal.science/hal-04243143v1>

Submitted on 2 May 2024

HAL is a multi-disciplinary open access archive for the deposit and dissemination of scientific research documents, whether they are published or not. The documents may come from teaching and research institutions in France or abroad, or from public or private research centers.

L'archive ouverte pluridisciplinaire **HAL**, est destinée au dépôt et à la diffusion de documents scientifiques de niveau recherche, publiés ou non, émanant des établissements d'enseignement et de recherche français ou étrangers, des laboratoires publics ou privés.

Fuzzy Fault-Tolerant Predefined-Time Control for Switched Systems: A Singularity-Free Method

Di Cui , Mohammed Chadli , *Senior Member, IEEE*, and Zhengrong Xiang , *Member, IEEE*

Abstract—The subject of this study is fuzzy predefined-time control for a class of switched nonlinear systems with multiple faults. In comparison to existing research on predefined-time control, this study delves into the realm of switched nonlinear systems, encompassing switched linear sensor faults and switched nonaffine faults. The difficulty in the controller design lies in following the backstepping technique, as taking the derivative of fractional power virtual control laws would trigger singularity issues at equilibrium states or coordinate transformation origins. The study utilizes the unique characteristics of switching and fuzzy logic systems to introduce a continuous piecewise predefined-time controller with a fault-tolerant compensation mechanism to avoid singularity problems. By adjusting a predefined parameter in the developed controller, the system could achieve the objectives of adaptive stability and adaptive tracking within a predefined time, as desired by the user. Moreover, the application of the proposed algorithm to practical systems is presented.

Index Terms—Adaptive fuzzy control, nonaffine faults, predefined-time control, sensor faults, switched nonlinear systems.

I. INTRODUCTION

DUE to the prevalence of nonlinear switched systems in practical applications, such as circuit systems [1], robotic manipulators [2], and computer disk drive systems [3], various control methods for switched nonlinear systems have been gaining increasing attention. The advantage of switched nonlinear systems lies in their combination of nonlinear and switching characteristics, which offers enhanced robustness and flexibility. When processing nonlinear functions, linear growth conditions are commonly used; however, such growth conditions make strong assumptions about the form of the function, thus limiting their ability to handle complex functions. In contrast, fuzzy logic systems (FLSs) offer greater flexibility and adaptability, enabling them to handle more complex nonlinear functions [4]. By designing fuzzy sets and fuzzy rules and utilizing fuzzy inference and defuzzification techniques, FLSs can approximate nonlinear functions more accurately. Furthermore, the robustness of

switched nonlinear systems can be further enhanced by integrating adaptive control methods [5], [6]. Therefore, the exploration of adaptive control for such systems has significant theoretical and practical value, leading to the publication of numerous outstanding results within the realm of adaptive control techniques for nonlinear switched systems [7], [8], [9], [10], [11], [12], [13]. For example, Zhang et al. [7] introduced an innovative state-dependent switching law, accompanied by a decentralized fuzzy controller, to effectively tackle the control challenges associated with switched interconnected nonlinear systems. Qi et al. [8] tackled the challenge of a switched boost converter circuit model suffering from random disturbances by devising an exquisite sliding mode controller under Markov switching and developing adaptive laws.

The escalating demands of industrial production have meant that people are increasingly striving to achieve faster implementation performance. To address this need, finite-time control theory was proposed [14], [15], [16], [17], [18], where systems can be quickly stabilized in finite time. For instance, for switched nonlinear uncertain stochastic systems, Li et al. [16] introduced a remarkable finite-time control scheme that leverages the synergistic power of command filters and adaptive fuzzy control. Their proposed approach ensures the convergence of switched nonlinear systems within the settling time. Notably, in finite-time stable systems, the maximum convergence time is typically dependent on the initial conditions. Specifically, as the norm of the initial values tends toward infinity, the maximum convergence time may also extend infinitely, thereby placing certain limitations on the system's performance. To overcome this limitation and further expedite the system's convergence, the fixed-time control approach was introduced and has gained widespread adoption. Within the framework of the fixed-time control scheme, the maximum convergence time remains unaffected by the initial values, which addresses the issue of unbounded convergence time [19], [20], [21], [22], [23]. For instance, a segmented terminal sliding mode fixed-time control strategy for a dc–dc buck converter system was developed in [19] to achieve superior tracking performance.

Although fixed-time stability surpasses finite-time stability in performance, establishing an immediate association between the settling time and tuning gains has been recognized as a complex task. Consequently, a novel concept known as predefined-time stability was extensively explored in [24]. This concept aims to overcome the aforementioned challenge by permitting an arbitrary selection of the settling time function's upper bound through the appropriate adjustment of the system's

This work was supported by the National Natural Science Foundation of China under Grant 62373191.

Di Cui and Zhengrong Xiang are with the School of Automation, Nanjing University of Science and Technology, Nanjing 210094, China (e-mail: cuidi19940725@gmail.com; xiangzr@mail.njust.edu.cn).

Mohammed Chadli is with the University Paris-Saclay, Univ Evry, IBISC, 91020 Evry, France (e-mail: mchadli20@gmail.com).

control parameters. This property proves to be particularly advantageous for systems exhibiting predefined-time stability [25], [26], [27], [28]. For instance, Mao et al. [27] developed a predefined-time consensus protocol for multi-agent systems using the sign function, guaranteeing that the multi-agent attains consensus within a predefined time. For switched nonlinear systems, the design and analysis of predefined-time control are more challenging due to the complexity of their dynamic characteristics and the presence of switching behavior. There are limited results currently available for predefined-time control of switched nonlinear systems. Further exploration in this direction would have potential research value.

On the other hand, the issue of faults in controlled systems is a widespread concern in industrial production. As the main components, if actuators or sensors fail, the system's performance and reliability would degrade and pose potential risks to personal safety, leading to production losses and significant economic implications. To mitigate the risks associated with sensor or actuator failures, employing fault-tolerant control (FTC) algorithms and strategies is crucial. Numerous FTC methods have been developed [29], [30], [31], [32], [33], [34]. For example, by employing adaptive technology and FLSs, a fixed-time FTC approach was developed for nonlinear systems with nonaffine faults in [29]. Furthermore, Liu et al. [34] tackled the intricate challenge of event-triggering FTC for microgrids with linear faults. Given the powerful combination of the backstepping strategy, the authors artfully designed a fault-tolerant consensus control protocol. However, it is vital to note that these existing control strategies predominantly focus on scenarios where either the systems are nonswitched or only a single fault type is considered. In addition, there is a dearth of research on how to establish a comprehensive predefined-time FTC approach for switched nonlinear systems that encompass multiple faults. This research gap is not only of great practical significance but also served as a source of inspiration for the current study.

Deriving inspiration from the insightful analyses presented earlier, this study addresses the issue of adaptive predefined-time fuzzy FTC for switched nonlinear systems in the presence of faults. The research makes multifaceted contributions, encompassing the following aspects.

- 1) A novel fuzzy predefined-time FTC strategy is devised. The application of the FLS not only facilitates the accomplishment of adaptive fuzzy control but also effectively addresses the challenge of nonaffine faults.
- 2) Unlike the predefined-time controllers outlined in [35] and [36], the continuous piecewise predefined-time controller proposed by this study not only enhances the convergence speed but also adeptly circumvents the singularity predicaments stemming from power exponent problems identified in previous works [35], [36].
- 3) Distinguished from the FTC strategies in [29], [32], and [37], the devised FTC method exhibits significant fault-tolerant capabilities in addressing sensor faults and non-affine faults subject to the switching law in this study by applying FLSs. Notably, systems afflicted by faults in [29], [30], and [38] can be considered special cases

within the broader framework of our system considered in this article.

The rest of this article is organized as follows. Section II is divided into two main parts. The first part focuses on the preparatory tasks for predefined-time control and FLSs, while the second part provides a comprehensive description of the switched nonlinear system with faults. In Section III, we present the developed predefined-time control method along with a detailed stability analysis. To validate the effectiveness of the designed controller, we simulate the switched resistor–inductor–capacitor (RLC) circuit and the switched continuous stirred tank reactor (CSTR) systems in Section IV. Finally, Section V concludes this article.

II. PRELIMINARIES AND PROBLEM FORMULATION

This section serves as a pivotal platform, provides a comprehensive definition of predefined time, and presents the relevant lemmas employed in deriving the predefined-time controller in Section A. Subsequently, the main research system and problem description are presented in Section B.

A. Preliminaries

Consider a nonlinear system as follows:

$$\dot{x} = h(x(t)), h(0) = 0, x(0) = 0 \quad (1)$$

where the origin is the equilibrium point, $x \in R^n$ is system state, and $h(x(t))$ is the system function.

Definition 1 (See [28]): If there is a positive constant δ , then, for $\forall x \in R^n$ and all $t \geq T_{\max} > 0$, satisfying $\|x(t)\| < \delta$, system (1) is practically predefined-time stable, with T_{\max} being a known predefined time.

Lemma 1 (See [28]): For the system (1), if $V(x(t)) > 0$ and $\dot{V}(x(t))$ meets

$$\dot{V}(x(t)) \leq -\frac{\pi}{c_0 T} \left(V^{1+\frac{c_0}{2}}(x(t)) + V^{1-\frac{c_0}{2}}(x(t)) \right) + b_0, t \geq 0$$

then, system (1) is practically predefined-time stable with $0 < c_0 < 1$, $T > 0$, and $d_0 > 0$. The predefined time is $2T$.

Lemma 2 (See [35]): For real numbers \mathcal{A} , \mathcal{B} , and l_0 , the following outcome holds true:

$$|\mathcal{P}|^{\mathcal{A}} |\mathcal{Q}|^{\mathcal{B}} \leq \frac{\mathcal{A} l_0}{\mathcal{A} + \mathcal{B}} |\mathcal{P}|^{\mathcal{A} + \mathcal{B}} + \frac{\mathcal{B} l_0^{-\frac{\mathcal{A}}{\mathcal{B}}}}{\mathcal{A} + \mathcal{B}} |\mathcal{Q}|^{\mathcal{A} + \mathcal{B}}$$

with \mathcal{P} and \mathcal{Q} being variables.

In this article, the Type-I FLS, also known as a Mamdani system, is utilized for modeling and decision-making in uncertain and imprecise environments. Notably, Type-I FLSs have the capability to estimate unknown continuous functions through fuzzification, reasoning methods, and defuzzification.

A Type-I FLS can be represented as follows:

$$\aleph(\eta) = \sum_{j=1}^q \psi_j \left[\prod_{i=1}^n \mu_{F_i^j}(\eta_i) \right] / \sum_{j=1}^q \left[\prod_{i=1}^n \mu_{F_i^j}(\eta_i) \right].$$

Here, the terms and symbols are defined as follows.

- 1) q is the number of fuzzy rules (i.e., if η_1 is F_1^j and \dots , and η_n is F_n^j , then \aleph is A^j).

2) A^j and F_i^j represent fuzzy sets with $\eta = [\eta_1, \dots, \eta_n]^T$.

3) $\mu_{F_i^j}$ expresses the fuzzy membership function.

4) $\psi_j = \max_{\eta \in \mathbb{R}} \mu_{A^j}(\mathbb{N})$ with $W = [\psi_1, \dots, \psi_q]^T$.

When $\varphi_j(\eta) = \prod_{i=1}^n \mu_{F_i^j}(\eta_i) / \sum_{j=1}^q [\prod_{i=1}^n \mu_{F_i^j}(\eta_i)]$ with $\varphi(\eta) = [\varphi_1(\eta), \dots, \varphi_q(\eta)]^T$, Type-I FLSs can be characterized as $\mathbb{N}(\eta) = \varpi^T \varphi(\eta)$.

Lemma 3 (See [29]): If the continuous function $\mathcal{H}(\eta)$ can be defined on $\Omega_\eta \subset R^q$, grounded on the universal approximation capability of Type-I FLSs, it is true that

$$\sup_{\eta \in \Omega_\eta} |\mathcal{H}(\eta) - \varpi^T \varphi(\eta)| \leq \nu$$

where ν represents the estimation error.

Remark 1: In the context of estimating unknown nonlinear functions, it is worth noting that Type-I FLSs have demonstrated a distinct advantage over Type-II FLSs. While Type-II FLSs offer advanced modeling capabilities for handling uncertainty, including modeling uncertainties within membership functions, they entail increased computational complexity and may necessitate a larger dataset for training and calibration. In our specific application, the inherent merits of Type-I FLSs, such as simplicity, interpretability, reduced computational load, and robustness, align well with our system's control and decision-making requirements.

Lemma 4 (See [35]): For $\mathfrak{S} > \tilde{\mathfrak{S}} > 0$, the following inequality holds:

$$\tilde{\mathfrak{S}}(\mathfrak{S} - \tilde{\mathfrak{S}})^\iota \leq \frac{\iota}{\iota + 1} (\mathfrak{S}^{\iota+1} - \tilde{\mathfrak{S}}^{\iota+1})$$

where $\iota > 1$.

Lemma 5 (See [39]): For any χ and $\varepsilon \in R$

$$0 \leq |\varepsilon| - \frac{\varepsilon^2}{\sqrt{\varepsilon^2 + \chi^2}} \leq \chi$$

where $\chi > 0$ and $\varepsilon > 0$.

B. System Description

Consider the following switched nonlinear systems subject to faults:

$$\begin{cases} \dot{x}_i(t) = x_{i+1}(t) + h_i^{\sigma(t)}(\bar{x}_i(t)) \\ \dot{x}_n(t) = u(t) + h_n^{\sigma(t)}(\bar{x}_n(t)) \\ \quad + \mathcal{L}(t - T_0) \mathcal{F}^{\sigma(t)}(\bar{x}_n(t), u(t)) \\ y^f(t) = x_1(t) \end{cases} \quad (2)$$

where $\bar{x}_i(t) = [x_1(t), x_2(t), \dots, x_i(t)]^T$ is the state vector; $h_i^{\sigma(t)}(\bar{x}_i(t))$ is a nonlinear continuous function under the switching law $\sigma(t) : [0, +\infty) \rightarrow \mathbb{M} = \{1, 2, \dots, m\}$; and $y^f(t)$ is the system output with sensor faults modeled as

$$y^f(t) = \beta^{\sigma(t)}(t)x_1(t) + \phi^{\sigma(t)}(t)$$

where $\beta^{\sigma(t)}(t)$ ($0 < \bar{\beta} \leq \beta^{\sigma(t)} \leq 1$) and $\phi^{\sigma(t)}(t)$ ($|\phi^{\sigma(t)}(t)| \leq \bar{\phi}$) are unknown continuous differentiable fault functions, and $\bar{\beta}$ and $\bar{\phi}$ are constants. When $\beta^{\sigma(t)}(t) = 1$ and $\phi^{\sigma(t)}(t) = 0$, it indicates that the sensor is functioning correctly. $\mathcal{F}^{\sigma(t)}(\bar{x}_n(t), u(t))$ denotes the unknown nonaffine switched fault with the system

input $u(t)$. The term $\mathcal{L}(t - T_0)$, which represents time-based characteristics of faults, can be described as

$$\mathcal{L}(t - T_0) = \begin{cases} 0, & t < T_0 \\ 1 - e^{-\mathcal{L}(t - T_0)}, & t \geq T_0 \end{cases}$$

where $|h_n^{\sigma(t)}(\bar{x}_n(t)) + \mathcal{L}(t - T_0) \mathcal{F}^{\sigma(t)}(\bar{x}_n(t), u(t))| \leq \mathcal{G}^{\sigma(t)}(\bar{x}_n(t), u(t))$, with $\mathcal{G}^{\sigma(t)}(\bar{x}_n(t), u(t))$ being an unknown non-negative function and $\mathcal{L} > 0$.

Remark 2: Despite there being several FTC strategies for mitigating actuator or sensor faults, this study addresses both switched nonaffine faults related to the input and switched sensor faults. In addition, the sensor faults we considered include the following.

- 1) $0 < \bar{\beta} \leq \beta^{\sigma(t)}(t) < 1$ and $\phi^{\sigma(t)}(t) = 0$ stand for the partial sensor failure.
- 2) $\beta^{\sigma(t)}(t) = 1$ and $\phi^{\sigma(t)}(t) = c$ (c is constant) represent the fixed bias fault.
- 3) $\beta^{\sigma(t)}(t) = 1$ and $|\dot{\phi}^{\sigma(t)}(t)| = dt$ ($0 < d \ll 1$) signify the drift fault.
- 4) $\beta^{\sigma(t)}(t) = 1$, $|\phi^{\sigma(t)}(t)| < \bar{\phi}(t)$, and $\dot{\phi}^{\sigma(t)} \rightarrow 0$ denote the sensor precision decline.

Compared with the single sensor fault considered in [32] and [38] and the linear actuator fault considered in [31] and [37], the faults considered in this study are more complex. Therefore, the development of FTC in this study poses a greater challenge.

The main objective of this research is to introduce an exquisite adaptive predefined-time fuzzy FTC approach, designed to fulfill the following crucial criteria for the system described by system (2).

- 1) The output variable $y^f(t)$ achieves bounded tracking of the reference signal $y_d(t)$, with the order up to the n th being derivable.
- 2) The closed-loop signals exhibit practical predefined-time stability.

Remark 3: Although some nonsingular predefined-time control strategies have been developed (Here, singularity refers to the inability to obtain the virtual controller as ζ_i equals 0), the main differences and advantages of nonsingular predefined-time control approaches in this study are as follows.

- 1) Compared with the method employed in [27] and [39], which utilize the sign function to evade singularity issues, the approach proposed in this study eliminates chattering phenomenon.
- 2) Unlike the work in [25], which only guarantees that the tracking error converges within a predefined time, this study focuses on the predefined-time stability of all signals in the system, not just tracking errors.
- 3) While the work in [28] also employed a piecewise controller to address the singularity problem, it is crucial to highlight that the piecewise controller used by Wang et al. [28] is discontinuous. This discontinuity poses challenges in obtaining the derivatives of the virtual controller. Notably, previous works, such as [26] and [37], introduced continuous piecewise predefined-time controllers to handle singularity issues; however, the controllers proposed

in these studies introduce an additional term requiring separate treatment.

III. MAIN RESULTS

In this section, an adaptive fuzzy predefined-time controller is devised by adapting common Lyapunov functions and FLSs. To lay the groundwork, we will first introduce a pivotal coordinate transformation, defined as follows:

$$\zeta_1 = y^f - y_d \quad (3)$$

$$\zeta_i = x_i - \alpha_{i-1}. \quad (4)$$

Step 1: Considering (2)–(4), we get

$$\dot{\zeta}_1 = \beta^k(\alpha_1 + h_1^k + \zeta_2) + \dot{\beta}^k x_1 + \dot{\phi}^k - \dot{y}_d \quad (5)$$

where k represents that the k th subsystem is active. Next, construct the following Lyapunov function candidate:

$$V_1 = \frac{1}{2}\zeta_1^2 + \frac{1}{2r_1}\tilde{\omega}_1^T\tilde{\omega}_1 \quad (6)$$

where $\tilde{\omega}_1 = \omega_1 - \hat{\omega}_1$.

Substituting (5) into (6) gives

$$\begin{aligned} \dot{V}_1 &\leq \zeta_1\beta^k(\alpha_1 + h_1^k + \zeta_2) + \frac{1}{r_1}\tilde{\omega}_1^T\dot{\tilde{\omega}}_1 \\ &\quad + \zeta_1\left(\dot{\beta}^k x_1 + \dot{\phi}^k - \dot{y}_d\right) \\ &\leq \zeta_1(\beta^k\alpha_1 + H_1^k(X_1) + \beta^k\zeta_2) - \frac{1}{r_1}\tilde{\omega}_1^T\dot{\tilde{\omega}}_1 - \zeta_1^2 \end{aligned} \quad (7)$$

where $H_1^k(X_1) = \beta^k h_1^k(\bar{x}_1) + \dot{\beta}^k x_1 + \zeta_1 + \dot{\phi}^k - \dot{y}_d$, $X_1 = [x_1, y_r, \dot{y}_d]^T$.

Applying Young's inequality obtains

$$\beta^k\zeta_1\zeta_2 \leq \frac{1}{2}\zeta_1^2 + \frac{1}{2}\zeta_2^2. \quad (8)$$

Type-I FLSs can estimate the unknown continuous function $H_1^k(X_1)$ with

$$H_1^k(X_1) = W_1^{kT}\varphi_1(X_1) + \nu_1(X_1)$$

where $\nu_1 \leq \bar{\nu}_1$ with $\bar{\nu}_1$ being a positive constant. Further,

$$\zeta_1 H_1^k \leq \frac{\zeta_1^2}{2a_1}\varpi_1\varphi_1^T\varphi_1 + \frac{a_1^2}{2} + \frac{\zeta_1^2}{2} + \frac{\bar{\nu}_1^2}{2} \quad (9)$$

where $\varpi_1 = \max\{\|W_1^k\|^2, k \in \mathbb{M}\}$, and $a_1 > 0$ is a parameter.

The virtual controller α_1 and the adaptive rate $\hat{\omega}_1$ are designed as

$$\alpha_1 = -\frac{\zeta_1\vartheta_1^2}{\beta\sqrt{\zeta_1^2\vartheta_1^2 + \kappa_1^2}} \quad (10)$$

$$\vartheta_1 = \frac{\Gamma_1}{\Gamma_2}\zeta_1^{\frac{c_2+c_1}{c_2}} + \frac{\Gamma_3}{\Gamma_4}\zeta_1 + \frac{\zeta_1}{2a_1^2}\hat{\omega}_1\varphi_1^T\varphi_1 \quad (11)$$

$$\dot{\hat{\omega}}_1 = \frac{r_1}{2a_1^2}\zeta_1^2\varphi_1^T\varphi_1 - \Gamma_1\hat{\omega}_1^{\frac{c_2+c_1}{c_2}} - \Gamma_3\hat{\omega}_1 \quad (12)$$

where $\Gamma_1 = n^{\frac{c_1}{2c_2}}\pi c_2/(c_1 T)$, $\Gamma_2 = 2^{1+\frac{c_1}{2c_2}}$, $\Gamma_3 = \pi c_2/(c_1 T)$, $\Gamma_4 = 2^{1-\frac{c_1}{2c_2}}$, $r_1 > 0$, $\kappa_1 > 0$, and $0 < c_1 < c_2 < 1$. c_1 and c_2

are odd integers and

$$\varsigma_1 = \begin{cases} \zeta_1^{\frac{c_2-c_1}{c_2}}, & |\zeta_1| \geq \xi_1 \\ \xi_1^{-\frac{2c_2-c_1}{c_2}}(2+\frac{c_1}{2c_2})\zeta_1^3 - \xi_1^{-\frac{4c_2-c_1}{c_2}}(1+\frac{c_1}{2c_2})\zeta_1^5, & |\zeta_1| < \xi_1. \end{cases}$$

Applying Lemma 5, we have

$$\begin{aligned} \zeta_1\beta^k\alpha_1 &\leq -\frac{\zeta_1^2\vartheta_1^2}{\sqrt{\zeta_1^2\vartheta_1^2 + \kappa_1^2}} \\ &\leq \kappa_1 - |\zeta_1\vartheta_1| \\ &\leq \kappa_1 - \zeta_1\vartheta_1. \end{aligned} \quad (13)$$

When $|\zeta_1| < \xi_1$, the following holds:

$$\begin{aligned} -\zeta_1\vartheta_1 &= -\frac{\Gamma_3}{\Gamma_4}\xi_1^{-2-\frac{c_1}{c_2}}\left(2+\frac{c_1}{2c_2}\right)\zeta_1^4 - \frac{\Gamma_1}{\Gamma_2}\zeta_1^{2+\frac{c_1}{c_2}} \\ &\quad + \frac{\Gamma_3}{\Gamma_4}\xi_1^{-4-\frac{c_1}{c_2}}\left(1+\frac{c_1}{2c_2}\right)\zeta_1^6 - \frac{\zeta_1^2}{2a_1^2}\hat{\omega}_1\varphi_1^T\varphi_1 \\ &\leq -\frac{\Gamma_3}{\Gamma_4}\left(\xi_1^{-2-\frac{c_1}{c_2}}\left(2+\frac{c_1}{2c_2}\right)\zeta_1^4\right) - \frac{\zeta_1^2}{2a_1^2}\hat{\omega}_1\varphi_1^T\varphi_1 \\ &\quad + \frac{\Gamma_3}{\Gamma_4}\left(\xi_1^{-2-\frac{c_1}{c_2}}\left(1+\frac{c_1}{2c_2}\right)\zeta_1^4\right) - \frac{\Gamma_1}{\Gamma_2}\zeta_1^{2+\frac{c_1}{c_2}} \\ &\leq -\frac{\Gamma_3}{\Gamma_4}\xi_1^{-2-\frac{c_1}{c_2}}\zeta_1^4 - \frac{\Gamma_1}{\Gamma_2}\zeta_1^{2+\frac{c_1}{c_2}} - \frac{\zeta_1^2}{2a_1^2}\hat{\omega}_1\varphi_1^T\varphi_1 \\ &\leq -\frac{\Gamma_3}{\Gamma_4}\zeta_1^{2-\frac{c_1}{c_2}} - \frac{\Gamma_1}{\Gamma_2}\zeta_1^{2+\frac{c_1}{c_2}} \\ &\quad - \frac{\zeta_1^2}{2a_1^2}\hat{\omega}_1\varphi_1^T\varphi_1 + \frac{\Gamma_3}{\Gamma_4}\xi_1^{2-\frac{c_1}{c_2}}. \end{aligned} \quad (14)$$

Similarly, $-\zeta_1\vartheta_1 \leq -\frac{\Gamma_3}{\Gamma_4}\zeta_1^{2-\frac{c_1}{c_2}} - \frac{\Gamma_1}{\Gamma_2}\zeta_1^{2+\frac{c_1}{c_2}} - \frac{\zeta_1^2}{2a_1^2}\hat{\omega}_1\varphi_1^T\varphi_1$, when $|\zeta_1| \geq \xi_1$.

From (8)–(13), when $|\zeta_1| < \xi_1$, (7) can be rewritten as

$$\begin{aligned} \dot{V}_1 &\leq \frac{\zeta_1^2}{2a_1}\varpi_1\varphi_1^T\varphi_1 + \frac{a_1^2}{2} + \frac{\zeta_1^2}{2} + \frac{\bar{\nu}_1^2}{2} \\ &\quad + \frac{1}{2}\zeta_1^2 + \frac{1}{2}\zeta_2^2 + \kappa_1 - \zeta_1^2 + \frac{\Gamma_3}{\Gamma_4}\xi_1^{2-\frac{c_1}{c_2}} \\ &\quad - \frac{1}{r_1}\tilde{\omega}_1^T\left(\frac{r_1}{2a_1^2}\zeta_1^2\varphi_1^T\varphi_1 - \Gamma_1\hat{\omega}_1^{1+\frac{c_1}{c_2}} - \Gamma_3\hat{\omega}_1\right) \\ &\quad - \zeta_1\left(\frac{\Gamma_1}{\Gamma_2}\zeta_1^{1+\frac{c_1}{c_2}} + \frac{\Gamma_3}{\Gamma_4}\zeta_1^{1-\frac{c_1}{c_2}} + \frac{\zeta_1\hat{\omega}_1\varphi_1^T\varphi_1}{2a_1^2}\right) \\ &\leq \frac{\zeta_2^2}{2} + \frac{\Gamma_1}{r_1}\tilde{\omega}_1^T\hat{\omega}_1^{1+\frac{c_1}{c_2}} + \frac{\Gamma_3}{r_1}\tilde{\omega}_1^T\hat{\omega}_1 + \frac{\Gamma_3}{\Gamma_4}\zeta_1^{2-\frac{c_1}{c_2}} \\ &\quad - \frac{\Gamma_1}{\Gamma_2}\zeta_1^{2+\frac{c_1}{c_2}} - \frac{\Gamma_3}{\Gamma_4}\zeta_1^{2-\frac{c_1}{c_2}} + \frac{a_1^2}{2} + \frac{\bar{\nu}_1^2}{2} + \kappa_1. \end{aligned} \quad (15)$$

When $|\zeta_1| < \xi_1$, (7) can be rewritten as

$$\begin{aligned} \dot{V}_1 &\leq \frac{\zeta_2^2}{2} + \frac{\Gamma_1}{r_1}\tilde{\omega}_1^T\hat{\omega}_1^{1+\frac{c_1}{c_2}} + \frac{\Gamma_3}{r_1}\tilde{\omega}_1^T\hat{\omega}_1 + \frac{a_1^2}{2} + \frac{\bar{\nu}_1^2}{2} \\ &\quad - \frac{\Gamma_1}{\Gamma_2}\zeta_1^{2+\frac{c_1}{c_2}} - \frac{\Gamma_3}{\Gamma_4}\zeta_1^{2-\frac{c_1}{c_2}} + \kappa_1. \end{aligned} \quad (16)$$

Implementing Lemmas 2 and 4 gives

$$\frac{\Gamma_1}{r_1} \tilde{\omega}_1^T \tilde{\omega}_1^{1+\frac{c_1}{c_2}} \leq \frac{\Gamma_1}{r_1} \frac{c_2 + c_1}{2c_2 + c_1} \left(\varpi_1^{2+\frac{c_1}{c_2}} - \tilde{\omega}_1^{2+\frac{c_1}{c_2}} \right) \quad (17)$$

$$\frac{\Gamma_3}{r_1} \tilde{\omega}_1^T \tilde{\omega}_1 \leq \frac{\Gamma_3}{2r_1} (\varpi_1^2 - \tilde{\omega}_1^2) \quad (18)$$

$$\left(\frac{1}{2r_1} \tilde{\omega}_1^2 \right)^{\frac{2c_2-c_1}{2c_2}} \leq \left(\frac{1}{2r_1} \tilde{\omega}_1^2 \right) + \frac{c_1}{2c_2} \left(\frac{2c_2 - c_1}{2c_2} \right)^{\frac{2c_2-c_1}{c_1}}. \quad (19)$$

Then, \dot{V}_1 can be written as

$$\begin{aligned} \dot{V}_1 \leq & -\Gamma_2 \Gamma_1 \frac{c_2 + c_1}{2c_2 + c_1} \left(\frac{1}{2r_1} \tilde{\omega}_1^2 \right)^{1+\frac{c_1}{2c_2}} \\ & - \Gamma_1 \left(\frac{1}{2} \zeta_1^2 \right)^{1+\frac{c_1}{2c_2}} - \Gamma_3 \left(\frac{1}{2} \zeta_1^2 \right)^{1-\frac{c_1}{2c_2}} \\ & + \Delta_1 + \frac{\zeta_2^2}{2} - \Gamma_3 \left(\frac{1}{2r_1} \tilde{\omega}_1^2 \right)^{\frac{2c_2-c_1}{2c_2}} \end{aligned} \quad (20)$$

where $\Xi_1 = \frac{a_1^2}{2} + \frac{\bar{\nu}_1^2}{2} + \kappa_1 + \frac{\Gamma_1}{r_1} \frac{c_2+c_1}{2c_2+c_1} \varpi_1^{2+\frac{c_1}{c_2}} + \frac{\Gamma_3}{2r_1} \varpi_1^2 + \frac{\Gamma_3 c_1}{2c_2} \left(\frac{2c_2-c_1}{2c_2} \right)^{\frac{2c_2-c_1}{c_1}}$ with

$$\Delta_1 = \begin{cases} \Xi_1 & |\zeta_1| \geq \xi_1 \\ \Xi_1 + \frac{\Gamma_3}{\Gamma_4} \xi_1^{2-\frac{c_1}{c_2}} & |\zeta_1| < \xi_1. \end{cases}$$

Step i ($2 \leq i \leq n-1$): Choose the following Lyapunov function candidate:

$$V_i = V_{i-1} + \frac{1}{2} \zeta_i^2 + \frac{1}{2r_i} \tilde{\omega}_i^T \tilde{\omega}_i \quad (21)$$

where $\tilde{\omega}_i = \varpi_i - \hat{\omega}_i$.

Computing the derivative of the V_i function results in

$$\begin{aligned} \dot{V}_i \leq & \dot{V}_{i-1} + \zeta_i (\alpha_i + h_i^k + \zeta_{i+1} - \dot{\alpha}_{i-1}) + \frac{1}{r_i} \tilde{\omega}_i^T \dot{\tilde{\omega}}_i \\ \leq & \dot{V}_{i-1} + \zeta_i H_i^k(X_i) + \zeta_i \alpha_i + \frac{1}{2} \zeta_i^2 \\ & + \frac{1}{2} \zeta_{i+1}^2 - \frac{1}{r_i} \tilde{\omega}_i^T \dot{\tilde{\omega}}_i - \frac{3}{2} \zeta_i^2 \end{aligned} \quad (22)$$

where $X_i = [x_1, \dots, x_i, \hat{\omega}_1, \dots, \hat{\omega}_i, y_d, \dot{y}_d, \dots, y_d^{(i)}]^T$, and $H_i^k(X_i) = h_i^k + \frac{3}{2} \zeta_i - \dot{\alpha}_{i-1}$. Type-I FLSs are introduced to estimate the unknown continuous function $H_i^k(X_i)$ with

$$H_i^k(X_i) = W_i^{kT} \varphi_i(X_i) + \nu_i(X_i)$$

where $\nu_i \leq \bar{\nu}_i$, and $\bar{\nu}_i$ is a positive constant. Then,

$$\zeta_i H_i^k \leq \frac{\zeta_i^2}{2a_i^2} \varpi_i \varphi_i^T \varphi_i + \frac{a_i^2}{2} + \frac{\zeta_i^2}{2} + \frac{\bar{\nu}_i^2}{2} \quad (23)$$

where $\varpi_i = \max\{\|W_i^k\|^2, k \in \mathbb{M}\}$, and $a_i > 0$ is a parameter.

The virtual controller α_i and the adaptive rate $\hat{\omega}_i$ are designed as

$$\alpha_i = - \frac{\zeta_i \vartheta_i^2}{\sqrt{\zeta_i^2 \vartheta_i^2 + \kappa_i^2}} \quad (24)$$

$$\vartheta_i = \frac{\Gamma_1}{\Gamma_2} \zeta_i^{1+\frac{c_1}{c_2}} + \frac{\Gamma_3}{\Gamma_4} \zeta_i + \frac{\zeta_i}{2a_i^2} \tilde{\omega}_i \varphi_i^T \varphi_i \quad (25)$$

$$\dot{\tilde{\omega}}_i = \frac{r_i}{2a_i^2} \zeta_i^2 \varphi_i^T \varphi_i - \Gamma_1 \tilde{\omega}_i^{1+\frac{c_1}{c_2}} - \Gamma_3 \tilde{\omega}_i \quad (26)$$

where $r_i > 0$, $\kappa_i > 0$, and

$$\zeta_i = \begin{cases} \zeta_i^{1-\frac{c_1}{c_2}}, & |\zeta_i| \geq \xi_i \\ \zeta_i^{-2-\frac{c_1}{c_2}} (2 + \frac{c_1}{2c_2}) \zeta_i^3 - \xi_i^{-4-\frac{c_1}{c_2}} (1 + \frac{c_1}{2c_2}) \zeta_i^5, & |\zeta_i| < \xi_i. \end{cases}$$

Applying the Lemma 5, repeating the steps of the first phase yields

$$\begin{aligned} \zeta_i \alpha_i \leq & - \frac{\zeta_i^2 \vartheta_i^2}{\sqrt{\zeta_i^2 \vartheta_i^2 + \kappa_i^2}} \\ \leq & \kappa_i - \zeta_i \vartheta_i \\ \leq & \kappa_i - \frac{\Gamma_3}{\Gamma_4} \zeta_i^{2-\frac{c_1}{c_2}} - \frac{\Gamma_1}{\Gamma_2} \zeta_i^{2+\frac{c_1}{c_2}} - \frac{\zeta_i^2}{2a_i^2} \tilde{\omega}_i \varphi_i^T \varphi_i. \end{aligned} \quad (27)$$

When $|\zeta_i| < \xi_i$, in order to avoid singularity problems, $\zeta_i \alpha_i$ satisfies $\zeta_i \alpha_i \leq \kappa_i - \frac{\Gamma_3}{\Gamma_4} \zeta_i^{2-\frac{c_1}{c_2}} - \frac{\Gamma_1}{\Gamma_2} \zeta_i^{2+\frac{c_1}{c_2}} - \frac{\zeta_i^2}{2a_i^2} \tilde{\omega}_i \varphi_i^T \varphi_i + \frac{\Gamma_3}{\Gamma_4} \xi_i^{2-\frac{c_1}{c_2}}$.

Further, when $|\zeta_i| \geq \xi_i$, (22) can be rewritten as

$$\begin{aligned} \dot{V}_i \leq & \sum_{m=1}^i \frac{\Gamma_1}{r_m} \tilde{\omega}_m^T \tilde{\omega}_m^{1+\frac{c_1}{c_2}} + \sum_{m=1}^i \frac{\Gamma_3}{r_m} \tilde{\omega}_m^T \tilde{\omega}_m \\ & - \sum_{m=1}^i \frac{\Gamma_1 \zeta_m^{2+\frac{c_1}{c_2}}}{\Gamma_2} - \sum_{m=1}^i \frac{\Gamma_3 \zeta_m^{2-\frac{c_1}{c_2}}}{\Gamma_4} + \frac{\zeta_{i+1}^2}{2} \\ & + \sum_{m=1}^i \frac{a_{m-1}^2}{2} + \sum_{m=1}^i \frac{\bar{\nu}_{m-1}^2}{2} + \sum_{m=1}^i \kappa_m. \end{aligned} \quad (28)$$

Likewise, when $|\zeta_i| < \xi_i$, one has

$$\begin{aligned} \dot{V}_i \leq & \sum_{m=1}^i \frac{\Gamma_1}{r_m} \tilde{\omega}_m^T \tilde{\omega}_m^{1+\frac{c_1}{c_2}} + \sum_{m=1}^i \frac{\Gamma_3}{r_m} \tilde{\omega}_m^T \tilde{\omega}_m \\ & - \sum_{m=1}^i \frac{\Gamma_1 \zeta_m^{2+\frac{c_1}{c_2}}}{\Gamma_2} - \sum_{m=1}^i \frac{\Gamma_3 \zeta_m^{2-\frac{c_1}{c_2}}}{\Gamma_4} \\ & + \sum_{m=1}^i \frac{a_{m-1}^2}{2} + \sum_{m=1}^i \frac{\bar{\nu}_{m-1}^2}{2} + \sum_{m=1}^i \kappa_m \\ & + \sum_{m=1}^i \frac{\Gamma_3}{\Gamma_4} \xi_m^{2-\frac{c_1}{c_2}} + \frac{\zeta_{i+1}^2}{2}. \end{aligned} \quad (29)$$

Drawing from the preceding classification discussion and applying Lemmas 2 and 4, we can conclude that

$$\begin{aligned} \dot{V}_i \leq & - \sum_{m=1}^i \Gamma_2 \Gamma_1 \frac{c_2 + c_1}{2c_2 + c_1} \left(\frac{1}{2r_m} \tilde{\omega}_m^2 \right)^{1+\frac{c_1}{2c_2}} \\ & - \sum_{m=1}^i \Gamma_1 \left(\frac{1}{2} \zeta_m^2 \right)^{1+\frac{c_1}{2c_2}} - \sum_{m=1}^i \Gamma_3 \left(\frac{1}{2} \zeta_m^2 \right)^{1-\frac{c_1}{2c_2}} \end{aligned}$$

$$- \sum_{m=1}^i \Gamma_3 \left(\frac{1}{2r_m} \tilde{\omega}_m^2 \right)^{\frac{2-c_1}{2c_2}} + \Delta_i + \frac{\zeta_{i+1}^2}{2} \quad (30)$$

where $\Xi_i = \Xi_{i-1} + \frac{a_i^2}{2} + \frac{\bar{\nu}_i^2}{2} + \kappa_i + \frac{\Gamma_1}{r_i} \frac{c_2+c_1}{2c_2+c_1} \varpi_i^{2+\frac{c_1}{c_2}} + \frac{\Gamma_3}{2r_i} \varpi_i^2 + \frac{\Gamma_3 c_1}{2c_2} \left(\frac{2c_2-c_1}{2c_2} \right)^{\frac{2c_2-c_1}{c_1}}$ with

$$\Delta_i = \begin{cases} \Xi_i & |\zeta_i| \geq \xi_i \\ \Xi_i + \frac{\Gamma_3}{r_i} \zeta_i^{2-\frac{c_1}{c_2}} & |\zeta_i| < \xi_i. \end{cases}$$

Step n : Construct the Lyapunov function as

$$V_n = V_{n-1} + \frac{1}{2} \zeta_n^2 + \frac{1}{2r_n} \tilde{\omega}_n^T \tilde{\omega}_n. \quad (31)$$

Then, \dot{V}_n can be obtained as follows:

$$\begin{aligned} \dot{V}_n &\leq \dot{V}_{n-1} + \zeta_n (u + h_n^k - \dot{\alpha}_{n-1} + \mathcal{L}(t - T_0) \mathcal{F}^k(\bar{x}_n, u)) \\ &\quad + \frac{1}{r_n} \tilde{\omega}_n^T \dot{\tilde{\omega}}_n \\ &\leq \dot{V}_{n-1} + \zeta_n H_n^k(X_n, u) + \zeta_n u - \frac{1}{r_n} \tilde{\omega}_n^T \dot{\tilde{\omega}}_n - \frac{1}{2} \zeta_n^2 \end{aligned} \quad (32)$$

where $H_n^k(X_n, u) = \frac{1}{2} \zeta_n - \dot{\alpha}_{n-1} + \mathcal{G}^k(\bar{x}_n, u)$ and $X_n = [x_1, \dots, x_n, \hat{\omega}_1, \dots, \hat{\omega}_n, y_d, \dot{y}_d, \dots, y_d^{(n)}]^T$. To overcome the algebraic loop issue that emerges while utilizing Type-I FLSs to estimate the term $\mathcal{G}^k(\bar{x}_n, u)$, the filtered signal u^f is introduced by subjecting the actual control input u to a Butterworth low-pass filter (LPF) $H_L(s)$, thus ensuring that $u^f = H_L(s)u \approx u$. Then, $H_n(X_n, u)$ can be estimated by an FLS as follows:

$$H_n^k(X_n, u) = W_n^{kT} \varphi_n(X_n, u^f) + \nu_n$$

where $\nu_n \leq \bar{\nu}_n$ with $\bar{\nu}_n$ being a positive constant. Then,

$$\zeta_n H_n^k \leq \frac{\zeta_n^2}{2a_n^2} \varpi_n \varphi_n^T \varphi_n + \frac{a_n^2}{2} + \frac{\zeta_n^2}{2} + \frac{\bar{\nu}_n^2}{2} \quad (33)$$

where $\varpi_n = \max\{\|W_n^k\|^2, k \in \mathbb{M}\}$, and a_n is a positive constant.

The controller u and the adaptive rate $\dot{\hat{\omega}}_n$ are designed as

$$u = - \frac{\zeta_n \vartheta_n^2}{\sqrt{\zeta_n^2 \vartheta_n^2 + \kappa_n^2}} \quad (34)$$

$$\vartheta_n = \frac{\Gamma_1}{\Gamma_2} \zeta_n^{1+\frac{c_1}{c_2}} + \frac{\Gamma_3}{\Gamma_4} \zeta_n + \frac{\zeta_n}{2a_n^2} \tilde{\omega}_n \varphi_n^T \varphi_n \quad (35)$$

$$\dot{\hat{\omega}}_n = \frac{r_i}{2a_n^2} \zeta_n^2 \varphi_n^T \varphi_n - \Gamma_1 \hat{\omega}_n^{1+\frac{c_1}{c_2}} - \Gamma_3 \hat{\omega}_n \quad (36)$$

where $r_n > 0, \kappa_n > 0$, and

$$\zeta_n = \begin{cases} \zeta_n^{\frac{c_2-c_1}{c_2}}, & |\zeta_n| \geq \xi_n \\ \zeta_n^{-2-\frac{c_1}{c_2}} (2 + \frac{c_1}{2c_2}) \zeta_n^3 - \xi_n^{-4-\frac{c_1}{c_2}} (1 + \frac{c_1}{2c_2}) \zeta_n^5, & |\zeta_n| < \xi_n. \end{cases}$$

When $|\zeta_n| \geq \xi_n$, applying Lemma 5 allows us to stack the steps of the process at step i to conclude that

$$\begin{aligned} \zeta_n \alpha_n &\leq - \frac{\zeta_n^2 \vartheta_n^2}{\sqrt{\zeta_n^2 \vartheta_n^2 + \kappa_n^2}} \\ &\leq \kappa_n - |\zeta_n \vartheta_n| \end{aligned}$$

$$\leq \kappa_n - \frac{\Gamma_3}{\Gamma_4} \zeta_n^{2-\frac{c_1}{c_2}} - \frac{\Gamma_1}{\Gamma_2} \zeta_n^{2+\frac{c_1}{c_2}} - \frac{\zeta_n^2}{2a_n^2} \tilde{\omega}_n \varphi_n^T \varphi_n. \quad (37)$$

To avoid situations where a virtual controller cannot be obtained when the value of ζ_n is close to 0, we consider switching to another controller mode and obtain $\zeta_n \alpha_n \leq \kappa_n - \frac{\Gamma_3}{\Gamma_4} \zeta_n^{2-\frac{c_1}{c_2}} - \frac{\Gamma_1}{\Gamma_2} \zeta_n^{2+\frac{c_1}{c_2}} - \frac{\zeta_n^2}{2a_n^2} \tilde{\omega}_n \varphi_n^T \varphi_n + \frac{\Gamma_3}{\Gamma_4} \zeta_n^{2-\frac{c_1}{c_2}}$.

Further, applying Lemmas 2 and 4, (32) can be rewritten as

$$\begin{aligned} \dot{V}_n &\leq - \sum_{m=1}^n \Gamma_2 \Gamma_1 \frac{c_2 + c_1}{2c_2 + c_1} \left(\frac{1}{2r_m} \tilde{\omega}_m^2 \right)^{1+\frac{c_1}{2c_2}} \\ &\quad - \sum_{m=1}^n \Gamma_1 \left(\frac{1}{2} \zeta_m^2 \right)^{1+\frac{c_1}{2c_2}} - \sum_{m=1}^n \Gamma_3 \left(\frac{1}{2} \zeta_m^2 \right)^{1-\frac{c_1}{2c_2}} \\ &\quad - \sum_{m=1}^n \Gamma_3 \left(\frac{1}{2r_m} \tilde{\omega}_m^2 \right)^{\frac{2-c_1}{2c_2}} + \Delta_n \end{aligned} \quad (38)$$

where $\Xi_n = \Xi_{n-1} + \frac{a_n^2}{2} + \frac{\bar{\nu}_n^2}{2} + \kappa_n + \frac{\Gamma_1}{r_n} \frac{c_2+c_1}{2c_2+c_1} \varpi_n^{2+\frac{c_1}{c_2}} + \frac{\Gamma_3}{2r_n} \varpi_n^2 + \frac{\Gamma_3 c_1}{2c_2} \left(\frac{2c_2-c_1}{2c_2} \right)^{\frac{2c_2-c_1}{c_1}}$ with

$$\Delta_n = \begin{cases} \Xi_n & |\zeta_n| \geq \xi_n \\ \Xi_n + \frac{\Gamma_3}{\Gamma_4} \zeta_n^{2-\frac{c_1}{c_2}} & |\zeta_n| < \xi_n. \end{cases}$$

Theorem 1: If the nonlinear system in a switched nonlinear system (2) can be estimated by Type-I FLSs, for any bounded initial conditions, the stability of switched nonlinear system (2) with faults can be ensured under arbitrary switching laws by designing virtual controllers (10) and (24), actual controller (34), and update laws (12), (26), and (36). Moreover, the tracking error converges into a set within predefined time.

Proof: According to (38)

$$\begin{aligned} \dot{V} &\leq - \Gamma_1 n^{-\frac{c_1}{2c_2}} \left(\sum_{m=1}^n \left(\frac{1}{r_m} \tilde{\omega}_m^2 + \frac{1}{2} \zeta_m^2 \right) \right)^{1+\frac{c_1}{2c_2}} \\ &\quad - \Gamma_3 \left(\sum_{m=1}^n \left(\frac{1}{r_m} \tilde{\omega}_m^2 + \frac{1}{2} \zeta_m^2 \right) \right)^{1-\frac{c_1}{2c_2}} + \Delta_n \\ &\leq - \frac{c_1 \pi}{c_2 T} \left(V^{1+\frac{c_1}{2c_2}} + V^{1-\frac{c_1}{2c_2}} \right) + \Delta_n. \end{aligned} \quad (39)$$

From Lemma 1, the tracking error ζ_1 converges to

$$|\zeta_1| \leq \sqrt{\frac{2c_1 \Delta_n T}{c_2 \pi}}$$

with the predefined time $2T$.

IV. SIMULATION STUDIES

In this section, we present two examples—an RLC circuit system and a CSTR system—to empirically validate the theoretical findings presented in this study.

Example 1: An RLC circuit system [30] with three subsystems (refer to Fig. 1) is simulated in this section.

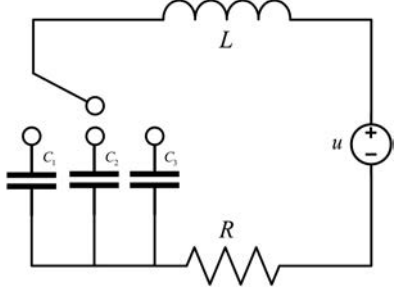


Fig. 1. Switched RLC circuit.

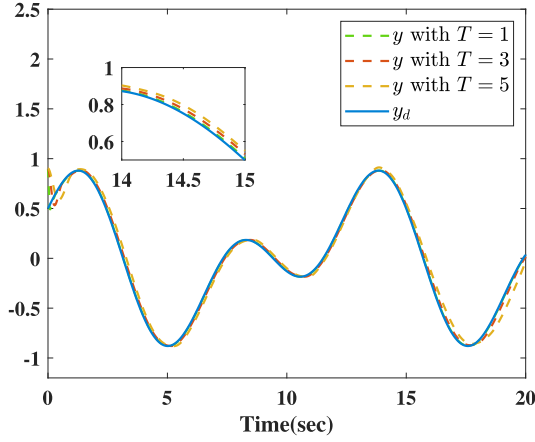


Fig. 2. Output and reference signal in Example 1.

Let the charge in the capacitor be x_1 and the flux in the inductance be x_2 . The RCL circuit system's dynamic becomes

$$\begin{cases} \dot{x}_1 = x_2 + \frac{1}{L}x_2 - x_2 \\ \dot{x}_2 = u - \frac{1}{C^{\sigma(t)}}x_1 - \frac{R}{L}x_2 + \mathcal{R}^{\sigma(t)} \end{cases} \quad (40)$$

where $\sigma(t) = \{1, 2, 3\}$, $C^1 = 100, C^2 = 75, C^3 = 50, L = 1.2$, and $R = 1$. $\mathcal{R}^{\sigma(t)} = \mathcal{L}(t - T_0)(Q^{\sigma(t)}x_1x_2 + \cos(u))$ is switched nonaffine faults and $Q^1 = 5, Q^2 = 6$, and $Q^3 = 7$. The sensor fault function is selected as

$$y^f = \begin{cases} x_1, & t < 8 \\ x_1 + 0.7, & t \geq 8. \end{cases}$$

The nonlinear fault function is selected as

$$\mathcal{L}(t - T_0) = \begin{cases} 0, & t < 11 \\ 1 - e^{-100(t-T_0)}, & t \geq 11. \end{cases}$$

Furthermore, the initial conditions are chosen as $[\hat{w}_1(0), \hat{w}_2(0), x_1(0), x_2(0)]^T = [0.9, 0.1, 1, 0.6]^T$. The Butterworth LPF is chosen as $H_L(s) = 1/(s^2 + 1.414s + 1)$, and the tracking signal is designated as $y_d = 0.5 \sin(t) + 0.5 \cos(0.5t)$. Let $c_1 = 3, c_2 = 5, \kappa_1 = 0.03, \kappa_2 = 0.05, r_1 = 5, r_2 = 6, a_1 = 5, a_2 = 4$, and $\beta_1 = 0.69$. To elaborate on the validity of the developed method, three groups of predefined times are considered: $2T = 2, 2T = 6$, and $2T = 10$.

The tracking performance is displayed in Fig. 2, under the switched rule in Fig. 3. We can see that, with the time T given in advance by humans, the system (40) could attain stability

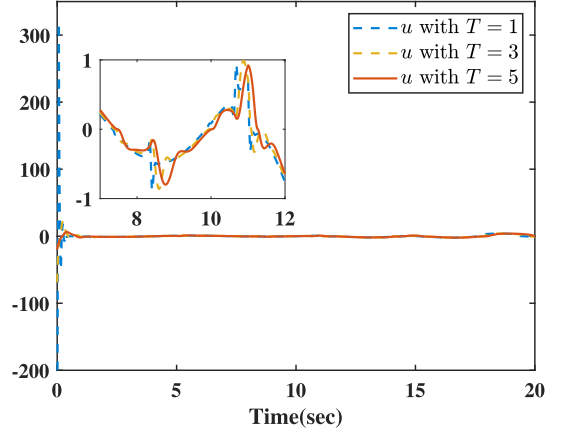


Fig. 3. Switching signal in Example 1.

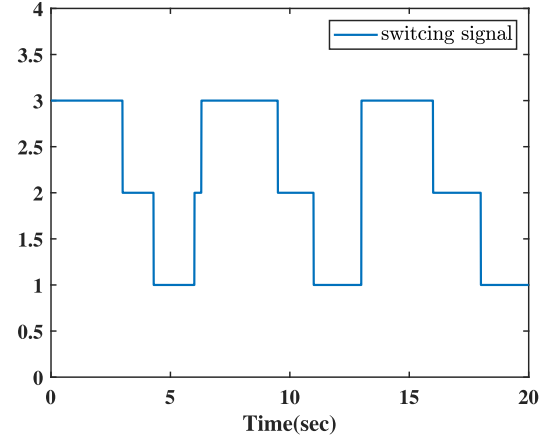


Fig. 4. Control input in Example 1.

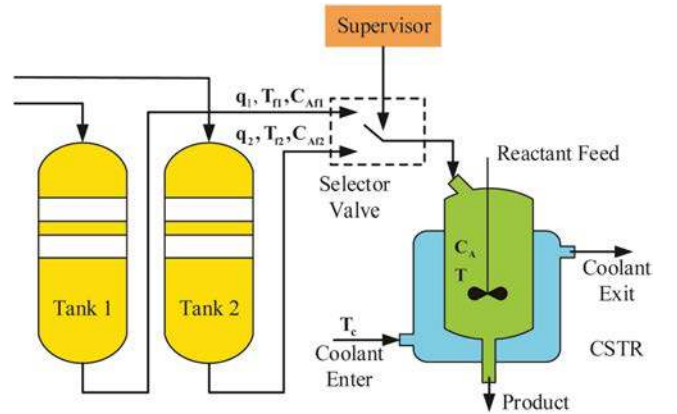


Fig. 5. Schematic of the process.

within $2T$ under the designed controller. Fig. 4 expresses the actual control signals under faults.

Example 2: A CSTR system with a consistent liquid volume (refer to Fig. 5) is examined in this part. The reactor is fed through an inlet stream that is controlled using a switching valve linked to two different input streams. The standard

TABLE I
NOMINAL PARAMETERS OF THE PROCESS

Parameter	Value
V	100 (L)
ρ	1000 ($g L^{-1}$)
C_p	0.239 ($J g^{-1} K^{-1}$)
ΔH	-5×10^4 ($J mol^{-1}$)
E/R	8750 (K)
k_0	7.2×10^{10} (min^{-1})
UA	5×10^4 ($J min^{-1} K^{-1}$)
$k_1 = \frac{\Delta H}{\rho C_p} k_0$	-1.506×10^{13}
$k_2 = \frac{UA}{V \rho C_p}$	2.092
q_1	50 ($L min^{-1}$)
q_2	200 ($L min^{-1}$)
C_{Af1}	1.5 ($mol L^{-1}$)
C_{Af2}	0.75 ($mol L^{-1}$)
T_{f1}	350 (K)
T_{f2}	350 (K)

operating conditions associated with an unstable equilibrium point for both modes are as follows: $T_1^* = 350$ K, $T_c^* = 300$ K, and $C_A^* = 0.5$ mol/L.

Table I provides the process parameters for the CSTR system [40]. The dynamic model of the CSTR system is obtained through energy balances and mass

$$\begin{aligned} \dot{C}_A &= \frac{q^{\sigma(t)}}{V} (C_{Af\sigma(t)} - C_A) - k_0 e^{(-\frac{E}{RT})} C_A \\ \dot{T}_1 &= \frac{q^{\sigma(t)}}{V} (T_{f\sigma(t)} - T_1) - k_1 e^{(-\frac{E}{RT})} C_A \\ &\quad + k_2 (T_c - T_1). \end{aligned} \quad (41)$$

Specify the states $x_1 = C_A - C_A^*$ and $x_2 = T_1 - T^*$. Then, (41) becomes

$$\begin{cases} \dot{x}_1 = x_2 + h_1^{\sigma(t)} \\ \dot{x}_2 = u + \mathcal{L}(t - T_0) \mathcal{F}^{\sigma(t)}(\bar{x}_n, u) \end{cases} \quad (42)$$

where $h_1^1 = 0.5x_1$, $h_1^2 = 2x_1$, and $\sigma(t) = \{1, 2\}$. The sensor fault function is selected as

$$y^f = \begin{cases} x_1, & t < 10 \\ (0.05e^{4-t} + 0.95)x_1, & t \geq 10. \end{cases}$$

The nonlinear fault function is selected as

$$\mathcal{L}(t - T_0) = \begin{cases} 0, & t < 17 \\ 1 - e^{-6(t-T_0)}, & t \geq 17 \end{cases}$$

with $\mathcal{F}^1(\bar{x}_2, u) = 0.5(x_1x_2 + \sin(u))$, $\mathcal{F}^2(\bar{x}_2, u) = 0.6(x_1x_2 + \sin(u))$, and the tracking signal is $y_d = \sin(t)$. Furthermore, the parameters in the adaptive law and controller are the same as in Example 1. The initial conditions are chosen as $[\hat{w}_1(0), \hat{w}_2(0), x_1(0), x_2(0)]^T = [0.5, 0.2, 0.7, 0.1]^T$.

The simulation results are presented in Figs. 6–9. The tracking performance is displayed in Fig. 6, under the switched rule in Fig. 8. Fig. 7 expresses the actual control signals under faults. The control input might have experienced a momentary surge due to the occurrence of faults; however, it quickly recovered and returned to a steady state. Moreover, four evaluation indices were considered [41]. The results in Fig. 9 further demonstrate that the

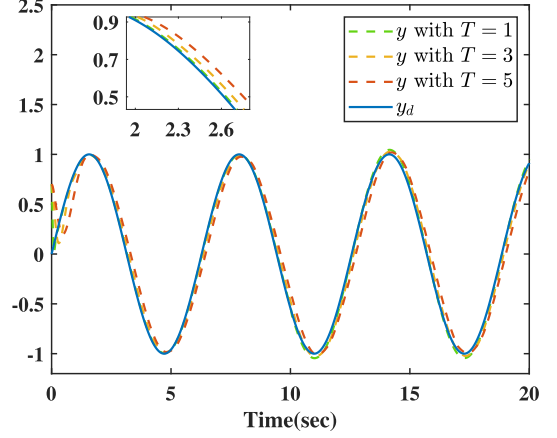


Fig. 6. Output and reference signal in Example 2.

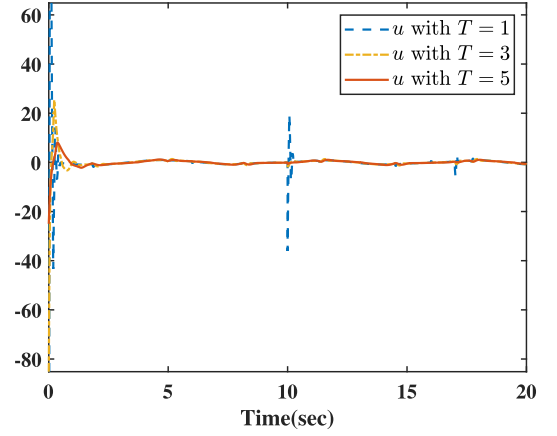


Fig. 7. Control input in Example 2.

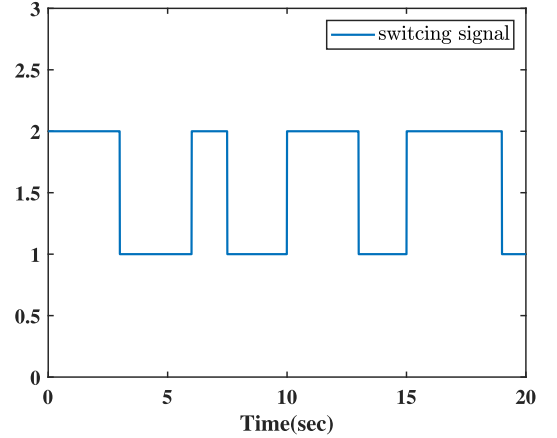


Fig. 8. Switching signal in Example 2.

tracking performance improved with a drop in T . Concurrently, there was a decline in robustness. Moreover, the energy consumption decreases as T increases, but the convergence accuracy is also decreased. Therefore, the choice of T needs to be made by accounting for the actual requirements and cost considerations in practical applications.

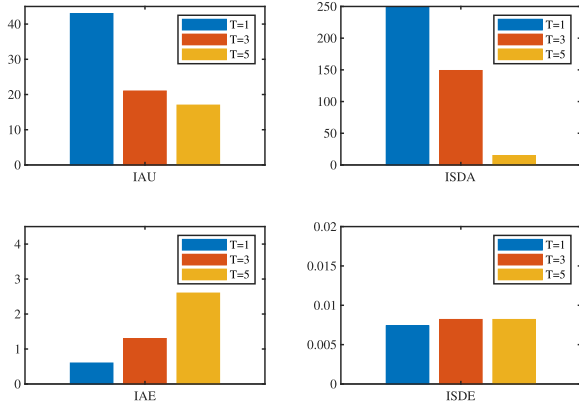


Fig. 9. Four evaluation indices under different predefined time in Example 2.

V. CONCLUSION

This article offers a discussion on the predefined-time adaptive fuzzy FTC tracking issue of switched nonlinear systems vulnerable to multiple faults. By relying on the strengths of FLSs, the designed predefined-time FTC scheme realized predefined-time tracking and robustness for multiple faults. The nonsingular predefined-time control approaches presented in this study demonstrate unique advantages and overcome the limitations encountered in existing methodologies. These refinements pave the way for developing more robust, precise, and computationally efficient control strategies, thereby enabling enhanced performance in practical systems, such as RLC and CSTR. In future studies, the application of the proposed control strategy to microgrids will be an engrossing subject. In addition, for further saving communication resources, event-triggered control methods [42], [43] will also be integrated into the proposed methods in the future.

REFERENCES

- [1] A. Fava, F. Centurelli, and G. Scotti, "A detailed model of cyclostationary noise in switched-resistor circuits," *IEEE Trans. Circuits Syst. I: Regular Papers*, vol. 70, no. 2, pp. 667–679, Feb. 2023.
- [2] D. Cheng, "Stabilization of planar switched systems," *Syst. Control Lett.*, vol. 51, no. 2, pp. 79–88, 2004.
- [3] T. Yamaguchi, H. Numasato, and H. Hirai, "A mode-switching control for motion control and its application to disk drives: Design of optimal mode-switching conditions," *IEEE/ASME Trans. Mechatron.*, vol. 3, no. 3, pp. 202–209, Sep. 1998.
- [4] H. Zhang, X. Guo, J. Sun, and Y. Zhou, "Event-triggered cooperative adaptive fuzzy control for stochastic nonlinear systems with measurement sensitivity and deception attacks," *IEEE Trans. Fuzzy Syst.*, vol. 31, no. 3, pp. 774–785, Mar. 2023.
- [5] Z. Feng, R.-B. Li, and L. Wu, "Adaptive decentralized control for constrained strong interconnected nonlinear systems and its application to inverted pendulum," *IEEE Trans. Neural Netw. Learn. Syst.*, early access, Jan 30, 2023, doi: 10.1109/TNNLS.2023.3238819.
- [6] W. Zou and J. Zhou, "A novel neural-network-based consensus protocol of nonlinear multiagent systems," *IEEE Trans. Autom. Control*, early access, doi: 10.1109/TAC.2023.3314653.
- [7] J. Zhang, S. Li, C. K. Ahn, and Z. Xiang, "Adaptive fuzzy decentralized dynamic surface control for switched large-scale nonlinear systems with full-state constraints," *IEEE Trans. Cybern.*, vol. 52, no. 10, pp. 10761–10772, Oct. 2022.
- [8] W. Qi, G. Zong, and W. X. Zheng, "Adaptive event-triggered SMC for stochastic switching systems with semi-Markov process and application to boost converter circuit model," *IEEE Trans. Circuits Syst. I: Regular Papers*, vol. 68, no. 2, pp. 786–796, Feb. 2021.
- [9] L. Long, F. Wang, and Z. Chen, "Robust adaptive dynamic event-triggered control of switched nonlinear systems," *IEEE Trans. Autom. Control*, vol. 68, no. 8, pp. 4873–4887, Aug. 2023, doi: 10.1109/TAC.2022.3217100.
- [10] S. Li, C. K. Ahn, J. Guo, and Z. Xiang, "Neural-network approximation-based adaptive periodic event-triggered output-feedback control of switched nonlinear systems," *IEEE Trans. Cybern.*, vol. 51, no. 8, pp. 4011–4020, 2021.
- [11] B. Niu, P. Duan, J. Li, and X. Li, "Adaptive neural tracking control scheme of switched stochastic nonlinear pure-feedback nonlower triangular systems," *IEEE Trans. Syst., Man, Cybern. Syst.*, vol. 51, no. 2, pp. 975–986, Feb. 2021.
- [12] X. Li and L. Long, "Distributed event-triggered fuzzy control of heterogeneous switched multi-agent systems under switching topologies," *IEEE Trans. Fuzzy Syst.*, early access, Aug. 07, 2023, doi: 10.1109/TFUZZ.2023.3302854.
- [13] S. Kamali, S. M. Tabatabaei, M. M. Arefi, and S. Yin, "Prescribed performance quantized tracking control for a class of delayed switched nonlinear systems with actuator hysteresis using a filter-connected switched hysteretic quantizer," *IEEE Trans. Neural Netw. Learn. Syst.*, vol. 33, no. 1, pp. 61–74, Jan. 2022.
- [14] T. Yang, H. Kang, H. Ma, and X. Wang, "Adaptive fuzzy finite-time fault-tolerant consensus tracking control for high-order multiagent systems with directed graphs," *IEEE Trans. Cybern.*, vol. 53, no. 1, pp. 607–616, Jan. 2023.
- [15] H. Li, C. Hua, K. Li, and Q. Li, "Finite-time control of high-order nonlinear random systems using state triggering signals," *IEEE Trans. Circuits Syst. I: Regular Papers*, vol. 70, no. 6, pp. 2587–2598, Jun. 2023.
- [16] S. Li, C. K. Ahn, and Z. Xiang, "Command-filter-based adaptive fuzzy finite-time control for switched nonlinear systems using state-dependent switching method," *IEEE Trans. Fuzzy Syst.*, vol. 29, no. 4, pp. 833–845, Apr. 2021.
- [17] W. Wei, T. Zhang, and W. Zhang, "Event-triggered finite-time adaptive practical tracking control for time-varying state-constrained nonlinear systems," *IEEE Trans. Fuzzy Syst.*, vol. 31, no. 5, pp. 1580–1592, May 2023.
- [18] S. Sui and S. Tong, "Finite-time fuzzy adaptive PPC for nonstrict-feedback nonlinear MIMO systems," *IEEE Trans. Cybern.*, vol. 53, no. 2, pp. 732–742, Feb. 2023.
- [19] Z. Liu et al., "Fixed-time sliding mode control for DC/DC buck converters with mismatched uncertainties," *IEEE Trans. Circuits Syst. I: Regular Papers*, vol. 70, no. 1, pp. 472–480, Jan. 2023.
- [20] B. Li, W. Gong, Y. Yang, B. Xiao, and D. Ran, "Appointed fixed time observer-based sliding mode control for a quadrotor UAV under external disturbances," *IEEE Trans. Aerosp. Electron. Syst.*, vol. 58, no. 1, pp. 290–303, Feb. 2022.
- [21] Y. Xie, Q. Ma, J. Gu, and G. Zhou, "Event-triggered fixed-time practical tracking control for flexible-joint robot," *IEEE Trans. Fuzzy Syst.*, vol. 31, no. 1, pp. 67–76, Jan. 2023.
- [22] W. Bai, P. X. Liu, and H. Wang, "Neural-network-based adaptive fixed-time control for nonlinear multiagent non-affine systems," *IEEE Trans. Neural Netw. Learn. Syst.*, early access, May 26, 2022, doi: 10.1109/TNNLS.2022.3175929.
- [23] S. Sui, C. L. P. Chen, and S. Tong, "A novel full errors fixed-time control for constraint nonlinear systems," *IEEE Trans. Autom. Control*, vol. 68, no. 4, pp. 2568–2575, Apr. 2023.
- [24] E. Jiménez-Rodríguez, A. J. Muñoz-Vázquez, J. D. Sánchez-Torres, M. Defoort, and A. G. Loukianov, "A Lyapunov-like characterization of predefined-time stability," *IEEE Trans. Autom. Control*, vol. 65, no. 11, pp. 4922–4927, Nov. 2020.
- [25] W. Shi, M. Hou, and G. Duan, "Prescribed-time asymptotic tracking control of strict feedback systems with time-varying parameters and unknown control direction," *IEEE Trans. Circuits Syst. I: Regular Papers*, vol. 69, no. 12, pp. 5259–5272, Dec. 2022.
- [26] H. Wang, M. Tong, X. Zhao, B. Niu, and M. Yang, "Predefined-time adaptive neural tracking control of switched nonlinear systems," *IEEE Trans. Cybern.*, vol. 53, no. 10, pp. 6538–6548, Oct. 2023, doi: 10.1109/TCYB.2022.3204275.
- [27] B. Mao, X. Wu, J. Lü, and G. Chen, "Predefined-time bounded consensus of multiagent systems with unknown nonlinearity via distributed adaptive fuzzy control," *IEEE Trans. Cybern.*, vol. 53, no. 4, pp. 2622–2635, Apr. 2023.
- [28] Q. Wang, J. Cao, and H. Liu, "Adaptive fuzzy control of nonlinear systems with predefined time and accuracy," *IEEE Trans. Fuzzy Syst.*, vol. 30, no. 12, pp. 5152–5165, Dec. 2022.

- [29] D. Cui, C. K. Ahn, and Z. Xiang, "Fault-tolerant fuzzy observer-based fixed-time tracking control for nonlinear switched systems," *IEEE Trans. Fuzzy Syst.*, early access, Jun. 12, 2023, doi: 10.1109/TFUZZ.2023.3284917.
- [30] L. Liu, Y.-J. Liu, D. Li, S. Tong, and Z. Wang, "Barrier Lyapunov function-based adaptive fuzzy FTC for switched systems and its applications to resistance–inductance–capacitance circuit system," *IEEE Trans. Cybern.*, vol. 50, no. 8, pp. 3491–3502, Aug. 2020.
- [31] L. Ma, N. Xu, X. Zhao, G. Zong, and X. Huo, "Small-gain technique-based adaptive neural output-feedback fault-tolerant control of switched nonlinear systems with unmodeled dynamics," *IEEE Trans. Syst., Man, Cybern. Syst.*, vol. 51, no. 11, pp. 7051–7062, Nov. 2021.
- [32] X. Wang, Y. Zhou, T. Huang, and P. Chakrabarti, "Event-triggered adaptive fault-tolerant control for a class of nonlinear multiagent systems with sensor and actuator faults," *IEEE Trans. Circuits Syst. I: Regular Papers*, vol. 69, no. 10, pp. 4203–4214, Oct. 2022.
- [33] H. J. Ma and L. X. Xu, "Decentralized adaptive fault-tolerant control for a class of strong interconnected nonlinear systems via graph theory," *IEEE Trans. Autom. Control*, vol. 66, no. 7, pp. 3227–3234, Jul. 2021.
- [34] G. Liu, Q. Sun, R. Wang, and H. Zhang, "Event-based fuzzy adaptive consensus FTC for microgrids with nonlinear item via prescribed fixed-time performance," *IEEE Trans. Circuits Syst. I: Regular Papers*, vol. 69, no. 7, pp. 2982–2993, Jul. 2022.
- [35] Y. Zhang, M. Chadli, and Z. Xiang, "Predefined-time adaptive fuzzy control for a class of nonlinear systems with output hysteresis," *IEEE Trans. Fuzzy Syst.*, vol. 31, no. 8, pp. 2522–2531, Aug. 2023, doi: 10.1109/TFUZZ.2022.3228012.
- [36] T. Zhang, S.-F. Su, W. Wei, and R.-H. Yeh, "Practically predefined-time adaptive fuzzy tracking control for nonlinear stochastic systems," *IEEE Trans. Cybern.*, early access, May 11, 2023, doi: 10.1109/TCYB.2023.3272581.
- [37] H. Wang, J. Ma, X. Zhao, B. Niu, M. Chen, and W. Wang, "Adaptive fuzzy fixed-time control for high-order nonlinear systems with sensor and actuator faults," *IEEE Trans. Fuzzy Syst.*, vol. 31, no. 8, pp. 2658–2668, Aug. 2023, doi: 10.1109/TFUZZ.2023.3235395.
- [38] L. Zhang and G.-H. Yang, "Observer-based fuzzy adaptive sensor fault compensation for uncertain nonlinear strict-feedback systems," *IEEE Trans. Fuzzy Syst.*, vol. 26, no. 4, pp. 2301–2310, Aug. 2018.
- [39] S. Xie and Q. Chen, "Adaptive nonsingular predefined-time control for attitude stabilization of rigid spacecrafts," *IEEE Trans. Circuits Syst. II: Exp. Briefs*, vol. 69, no. 1, pp. 189–193, Jan. 2022.
- [40] M. B. Yazdi and M. Jahed-Motlagh, "Stabilization of a CSTR with two arbitrarily switching modes using modal state feedback linearization," *Chem. Eng. J.*, vol. 155, no. 3, pp. 838–843, 2009.
- [41] J. Na, Q. Chen, X. Ren, and Y. Guo, "Adaptive prescribed performance motion control of servo mechanisms with friction compensation," *IEEE Trans. Ind. Electron.*, vol. 61, no. 1, pp. 486–494, Jan. 2014.
- [42] Y. Xu, T. Li, Y. Yang, S. Tong, and C. L. P. Chen, "Simplified ADP for event-triggered control of multiagent systems against FDI attacks," *IEEE Trans. Syst., Man, Cybern. Syst.*, vol. 53, no. 8, pp. 4672–4683, Aug. 2023.
- [43] Y. Xu, T. Li, Y. Yang, Q. Shan, S. Tong, and C. L. P. Chen, "Anti-attack event-triggered control for nonlinear multi-agent systems with input quantization," *IEEE Trans. Neural Netw. Learn. Syst.*, early access, Apr. 20, 2022, doi: 10.1109/TNNLS.2022.3164881.